Int J Clin Exp Med 2018;11(8):7680-7691
www.ijcem.com /ISSN:1940-5901/IJCEM0074682

Original Article

Inhibition of epirubicin poly (butyl cyanoacrylate) magnetic nanoparticles on tumor growth in rat livers: an experimental animal study

Jin-Zhu Wu[1*], Wei-Hua Cai[1], Ren-Fei Zhu[1], Chun-Yan Gu[2*], Liu-Cheng Wu[3*], Han-Zhen Ji[4*]

[1]Nantong Institute of Liver Disease, Department of Hepatobiliary Surgery, Nantong Third People's Hospital, Nantong University, Nantong, Jiangsu, China; [2]Center for Pathology, Department of Immunohistochemical Research, Nantong Third People's Hospital, Nantong University, Nantong, Jiangsu, China; [3]Nantong Institute of Comparative Medical Research, Laboratory Animal Center, Nantong University, Nantong, Jiangsu, China; [4]Hospital Library, Nantong Third People's Hosptial, Nantong University, Nantong, Jiangsu, China. [*]Equal contributors.

Received February 19, 2018; Accepted June 28, 2018; Epub August 15, 2018; Published August 30, 2018

Abstract: It has been reported that adriamycin magnetic nanoparticles can accumulate in tumor sites. The present study investigated the distribution of epirubicin poly (butyl cyanoacrylate) magnetic nanoparticles (EPI-PBCA-MNPS) in rat livers and its targetability. This study also explored whether EPI-PBCA-MNPS could inhibit the growth of orthotopically transplanted tumors of human liver cancer in nude mice under an applied magnetic field. A total of 75 SD rats in three groups were treated, respectively, with tail vein injections of EPI, EPI-PBCA-MNPS, and EPI-PBCA-MNPS, combined with an applied magnetic field (MF). Concentrations of epirubicin in the plasma, livers, hearts, lungs, spleens, and kidneys of SD rats in each group were measured. Results showed that the distribution of epirubicin in liver tissue under the environment of EPI-PBCA-MNPS+MF was highest. Peak concentration of epirubicin was advanced to 5 minutes after drug administration, indicating that EPI-PBCA-MNPS has a high targetability to the liver and the magnetic field plays a role in the orientation distribution of nanoparticles. A total of 40 nude mice were taken to be transplanted orthotopically with fresh human liver cancer in the liver parenchyma, establishing nude mouse models of human liver cancer. They were randomly divided into 4 groups with 10 mice in each group. Mice in the four groups were treated, respectively, with tail vein injections of normal saline (control group), EPI, EPI-PBCA-MNPS, and EPI-PBCA-MNPS, combined with an applied magnetic field. Experimental results showed that EPI-PBCA-MNPS can exert significant tumor inhibitory effects on orthotopically transplanted tumors of human liver cancer in nude mice and expression of proliferating cell nuclear antigens under an external magnetic field. This proves that EPI-PBCA-MNPS+MF can inhibit the cell cycle conversion of human liver cancer cells, *in vivo*, inhibiting the growth of liver cancer cells.

Keywords: Epirubicin poly (butyl cyanoacrylate) magnetic nanoparticles, liver cancer, mouse model of human liver cancer, target distribution

Introduction

Liver cancer is a common malignancy and liver-targeted drugs are a research hotspot [1]. The following two methods can be used to realize the target distribution of drugs in the liver. One method is that when the drug passes through the liposome carriers and nanocarriers, the phagocytosis in the reticular endothelial system is used to achieve drug targeting to the liver [2]. The second method is to link the drug to the carrier molecule and use hepatocyte receptor-mediated phagocytosis [3]. Epirubicin has no cell targetability and has greater toxic and side effects, thus its effects have been limited. However, epirubicin has better antitumor activity, markedly reducing its toxicity to the heart. To change the distribution of drugs in the body, the carrier system and the diameter of drug particles can be reduced to the nanometer scale to achieve a passive liver targeting effect [4]. Magnetic nanoparticles in targeted drug delivery systems are characterized by the fact that they can selectively arrive and locate in the target tumor region through blood vessels under guidance of an external magnetic field, slowly releasing the targeted drug from the carrier in a controlled manner. If the surface-modi-

fication of magnetic nanocarriers, such as linking magnetic nanocarriers to monoclonal antibodies, was conducted, the targetability of the magnetic nanocarriers will be stronger [5]. Targeting nanoparticle delivery systems has been extensively studied in the field of oncology [6-8]. Some studies have shown that nanoparticles have good passive targeting to the liver, in the 100-200 nm range, with no significant effects on drug loading capacity [9, 10]. In this study, the liver-targeting effects of epirubicin poly (butyl cyanoacrylate) magnetic nanoparticles (EPI-PBCA-MNPS, provided by National Key Laboratory Nanobiological Technology, Chinese Ministry of Health, nanoparticle size was 152.0±28.5 nm) were investigated [11]. Rats were injected intravenously with EPI-PBCA-MNPS through tail veins. In addition, an external magnetic field was placed around the liver tumors to observe the target distribution of EPI-PBCA-MNPS in the magnetic field environment. Nude mouse models bearing orthotopically transplanted tumors of human liver cancer were established. The effects of EPI-PBCA-MNPS on orthotopically transplanted tumors of human liver cancer in nude mice were observed. Related studies on anti-cancer mechanisms of epirubicin were carried out to provide a highly efficient new drug for targeted drug therapy of liver cancer.

Materials and methods

Detection of epirubicin concentrations in various organs

A total 75 SD rats were purchased and provided by the Animal Laboratory, Nanjing Biomedical Research Institute of Nanjing University (certificate number: 201604238). They were randomly divided into three groups. These included the EPI group (control group), EPI-PBCA-MNPS group, and EPI-PBCA-MNPS + magnetic field (MF) group, with 25 rats in each group. Tissue from the left lobe of the liver in rats of the EPI-PBCA-MNPS+MF group was taken as the tissue of target hepatic region and named as the target hepatic region group. Tissue from the right lobe of the liver in rats of the EPI-PBCA-MNPS+MF group was taken as the tissue of non-target hepatic region and named as non-target hepatic region group. Rats in the three groups were treated, respectively, with tail vein injections of EPI, EPI-PBCA-MNPS, and EPI-PBCA-MNPS (epirubicin dose in each group was 2.5 mg/kg), combined with an applied magnetic field. After successful anesthesia, the left lateral lobe of livers in rats of the EPI-PBCA-MNPS+MF group was exposed. A multifunctional vibrating sample magnetometer (VersaLab system, Quantum Design Inc, U.S.A.) with preset about 5000 Gs strong NdFeB magnet was placed in the left lateral lobe of livers of the rats. The linear regression equation was obtained by referring to the operating procedure described in the literature of Li et al. This was to determine the linear relationship between epirubicin concentration and fluorescence intensity [11, 12]. Five rats in each group were sacrificed by cervical spine fracture, respectively, at 5, 15, 30, 60 and 120 minutes after drug administration. Next, 2 mL blood was collected from the heart of each rat and centrifuged (6000 r/min) after anticoagulation to make plasma. In addition, organs such as hearts, lungs, livers, spleens, and kidneys were harvested. Blood on the organ surface was washed with normal saline and organs were then dried by filter papers. Subsequently, 1 g of tissue was taken from each organ (1 g tissue from left lobe of the liver in rats of EPI-PBCA-MNPS+MF group was taken as the target hepatic region group and 1 g tissue from the right lobe of the liver in rats of EPI-PBCA-MNPS+MF group was taken as the non-target hepatic region group) was weighed accurately to make the homogenate. Then, 6% hydrochloric acid alcohol was added to 1 mL plasma or 1 g homogenate to prepare the 5 mL solution. The solution was kept overnight and then centrifuged (16000 r/min) for 15 minutes to take l mL of supernatant. Ultraviolet-visible spectrophotometry (UV-5100) was used to detect fluorescence intensity. Concentrations of epirubicin in each organ were calculated according to the linear regression equation.

Preparation of orthotopically transplanted tumor of human liver cancer in nude mice

A total of 45 nude mice (male, animal laboratory of Nanjing University, Nanjing Institute of Biomedicine, certificate number: 201605762) and HepG2 human liver cancer cells (provided by Shanghai Institute of Biochemistry and Cell Biology, Chinese Academy of Sciences) were purchased. When HepG2 cells were cultured to be in the logarithmic growth phase, cell sus-

pension with a concentration of 5 × 10^7 cells/mL was prepared and inoculated into subcutaneous tissue at the neck and thigh in 5 nude mice, at a dose of 0.1 mL per site. When tumors grew to 1.5 cm in diameter, the orthotopic transplantation was performed [13]. Tumor tissue was placed in RPMI 1640 medium (Gibco) before inoculation and cut into approximately 1 mm × 1 mm tumor pieces for later use.

Establishment of nude mouse models of human liver cancer

Laparotomy was carried out in the remaining 40 nude mice after anesthesia. The left lobe of the liver was exposed and freshly resected human liver cancer was orthotopically transplanted into the liver parenchyma of the mouse with an anesthetic trocar, using intrahepatic tunnel implantation method. After hemostasis and suturing were performed, measures were taken to prevent incision infection.

Growth situation of live tumors in nude mice

After the mouse models of human liver cancer were established by surgery, the nude mice were randomly divided into 4 groups, with 10 mice in each group. Mice in the four groups were treated, respectively, with tail vein injections of normal saline (control group), EPI, EPI-PBCA-MNPS, and EPI-PBCA-MNPS, combined with an applied magnetic field. Except for the normal saline (NS) group (control group), the EPI dose for all mice in EPI group, EPI-PBCA-MNPS group, and EPI-PBCA-MNPS+MF group was 40 μg/mouse. The drug solution in three groups was diluted 3 times with normal saline. Mice were injected with 0.2 mL drug solution each time, successively through the tail veins. Then, a magnet (with diameter of 10 mm × 10 mm) was placed on the surface of tumors in mice of the EPI-PBCA-MNPS+MF group. The surface magnetic field strength was 5000 Gs and the magnet was fixed with an adhesive tape. The above operations were repeated once every three days, a total of three times. Growth of liver tumors in nude mice, before and after drug administration, was monitored and marked respectively by an ultrasonic dispersion instrument. Sizes, shapes, and metastasis situations of tumors in each group were monitored and measured by an ultrasonic dispersion instrument before the end of drug administration. When tumors grew up to a volume of 20-30 mm^3, they were cut along the longest axis, the growth of liver tumors and whether there was metastasis were further determined by the naked eye. The length (L) and width (w) of the sections were measured and tumor volume (V/mm^3) was calculated according to the following formula: $W^2 \times L \times 0.52$; tumor inhibition rate% = (1-the tumor volume in the experimental group/the tumor volume in the control group) × 100% [14]. After 2 weeks of treatment, the nude mice were dissected and the tumors were stripped and numbered. Tumor sizes were measured. Resected tumor specimens were fixed and embedded in paraffin. The remaining tumor specimens were cryopreserved in liquid nitrogen for further detecting the expression situation of tumors using Western blot and immunohistochemistry [15].

Western blot

Total protein was extracted from tumor tissue and protein concentrations were determined by the Bradford colorimetric method. Cell lysates with the same mass and an equal volume of 2 × electrophoresis loading buffer were added into the test tube. The test tube was placed in a boiling water bath for 3 minutes, followed by sample loading, electrophoresis, and transmembrane using the electrophoretic transfer apparatus. Membranes were then blocked with 5% skim milk for 1 hour at room temperature. The membranes were added with mouse anti human proliferating cell nuclear antigen (PCNA, Santa Cruz, California USA) and incubated overnight at 4°C. Subsequently, the membranes were washed three times with TBST and the solution was replaced once every 10 minutes. The membranes were added with alkaline phosphatase labeled secondary antibody and incubated for 45 minutes at 37°C. They were washed three times with TBST and the solution was replaced once every 15 minutes. The film was made in a dark room. Film development and fixing were carried out, along with gray-scale analysis using Image plus 5.0 software [16].

Immunohistochemistry

Paraffin-embedded tumor tissues were cut into sections at the same time. Each specimen wax block was cut into 3 sections with a thickness of 5 μm and tissue sections were dewaxed and hydrated. The tissue sections were pretreated

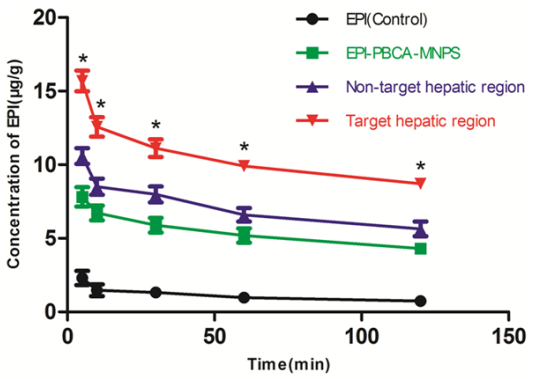

Figure 1. Concentrations of epirubicin in liver tissues of SD rats in three groups after intravenous injections of epirubicin through the tail vein After rats in three groups were treated respectively with tail vein injections of EPI, EPI-PBCA-MNPS, and EPI-PBCA-MNPS (the epirubicin dose in each group was 2.5 mg/kg), combined with applied magnetic field, peak drug concentrations in liver tissues were advanced to 5 minutes after tail vein drug administration. Concentrations of epirubicin in the liver tissue at different time points in the target hepatic region group were significantly higher than those in the non-target hepatic region group, EPI group, and EPI-BCA-MNPS group ($P < 0.05$), (*, $p < 0.05$) but there was no statistically significant difference between EPI-PSCA-MNPS group and non-target hepatic region group. Concentrations of epirubicin in the liver at different time points in the target hepatic region group were higher than those in non-target hepatic region group. Moreover, the ranking of concentrations of epirubicin in the liver at different time points in different groups from highest to lowest was as follows: the target hepatic region group > non-target hepatic region group > EPI-PSCA-MNPS group > EPI group (*, $p < 0.05$).

and rinsed in distilled water, then placed in TBS. Blockade of endogenous peroxidases was performed. Tissue sections were rinsed in distilled water and then placed in TBS for 10 minutes. Primary antibody was anti-PCNA antibody. Tissue sections were incubated with primary antibody for 10-30 minutes and then rinsed with TBS for 10 minutes. Tissue sections were incubated with EnVisionTM for 10-30 minutes and then rinsed with TBS for 10 minutes. Tissue sections were incubated with color-substrate solution for 10 minutes and then rinsed in distilled water, then counterstained and mounted [17]. Criteria for evaluation: percentage of positive cells with expression of PCNA in 50 high magnification lenses was counted at random. The number of positive cells less than 1% was set as 0 point, 1%-30% as 1 points, 31%-75% as 2 points, and more than 75% as 3 points; 0-3 points were recorded according to the depth of staining points, colorless specimens were considered as 0 points, light yellow specimens as 1 point, brown yellow specimens as 2 points, and brown specimens as 3 points. The two indicators were multiplied to record and evaluate results. A score of 0 points was recorded as (-), a score of ≤ 4 points was recorded as (+). Both were considered as negative expression of PCNA proteins. A score of > 4 and ≤ 6 was recorded as (++), a score of > 6 and ≤ 9 was recorded as (+++). Both were considered as positive expression of PCNA proteins [18].

Statistical analysis

All data are reported as mean ± standard error of the mean (SEM). Group means were compared by one-way ANOVA. Counting data were analyzed by X^2 test. All statistical analyses were performed with Prism 5.0 (GraphPad Software La Jolla, CA). A *p* value of less than 0.05 is considered statistically significant.

Results

Aggregation and target distribution of EPI-PSCA-MNPS

After rats in the three groups were treated, respectively, with tail vein injections of EPI, EPI-PBCA-MNPS, and EPI-PBCA-MNPS (epirubicin dose in each group was 2.5 mg/kg), combined with an applied magnetic field, the peak drug concentration in liver tissues was advanced to 5 minutes after drug administration and was highest in the target hepatic region group (15.70±1.56 μg/g). Concentrations of epirubicin in liver tissues at different time points in the target hepatic region group were significantly higher than those in the non-target hepatic region group, EPI group, and EPI-BCA-MNPS group ($p < 0.05$). There were no statistically significant differences between the EPI-PSCA-MNPS group and non-target hepatic region group. Concentrations of epirubicin at different time points in the target hepatic region group were higher than those in the non-target hepatic region group. Moreover, ranking of concentrations of epirubicin at different time points in the different groups, from highest to lowest, was as follows: the target hepatic region group > non-target hepatic region group > EPI-PSCA-MNPS group > EPI group, indicating that EPI-PBCA-MNPS had high drug targeting to the liver. The magnetic environment played a guiding

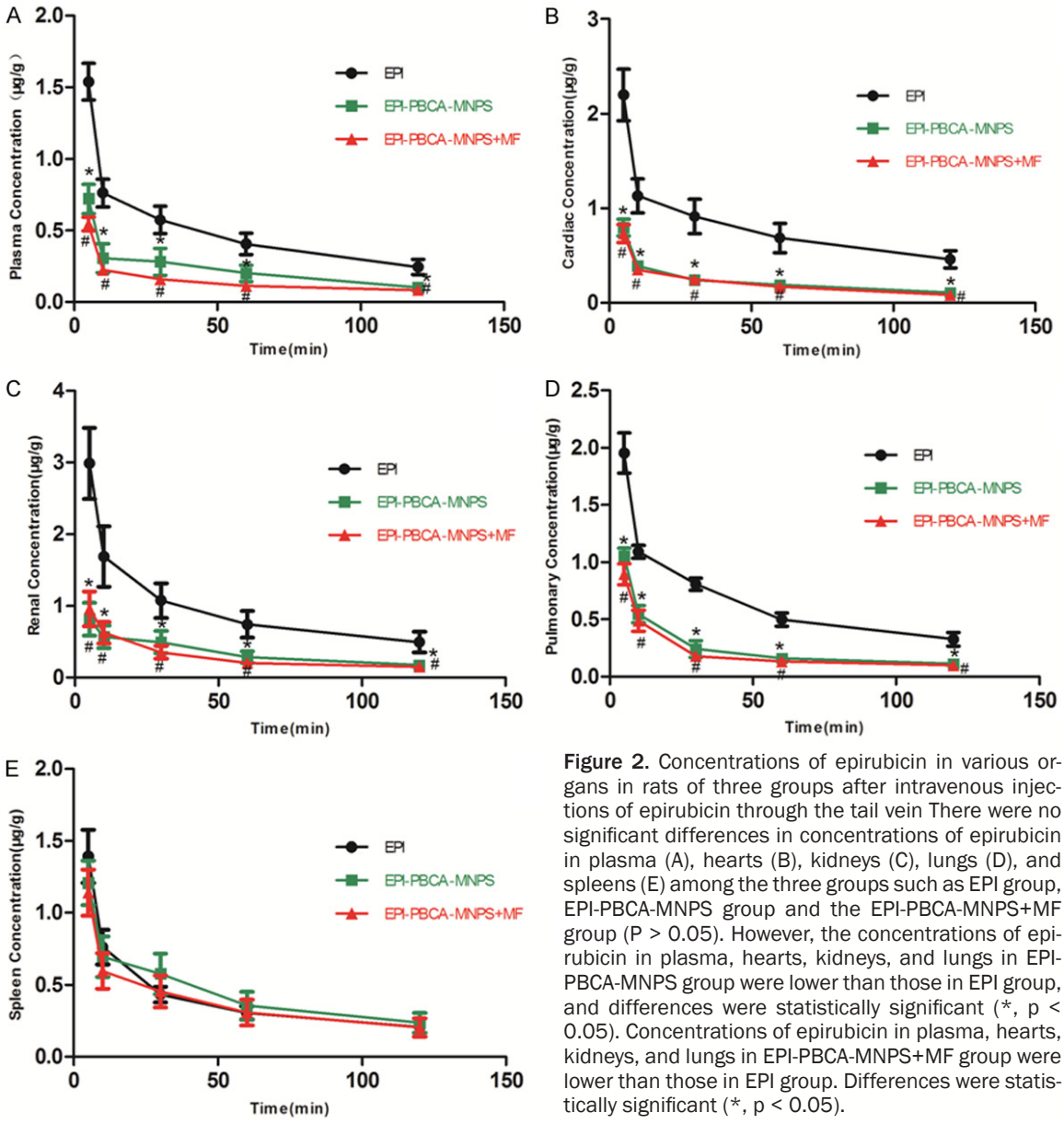

Figure 2. Concentrations of epirubicin in various organs in rats of three groups after intravenous injections of epirubicin through the tail vein There were no significant differences in concentrations of epirubicin in plasma (A), hearts (B), kidneys (C), lungs (D), and spleens (E) among the three groups such as EPI group, EPI-PBCA-MNPS group and the EPI-PBCA-MNPS+MF group ($P > 0.05$). However, the concentrations of epirubicin in plasma, hearts, kidneys, and lungs in EPI-PBCA-MNPS group were lower than those in EPI group, and differences were statistically significant (*, $p < 0.05$). Concentrations of epirubicin in plasma, hearts, kidneys, and lungs in EPI-PBCA-MNPS+MF group were lower than those in EPI group. Differences were statistically significant (*, $p < 0.05$).

role in localization and distribution of nanoparticles (**Figure 1**). The distribution of epirubicin in other extrahepatic organs, such as hearts, kidneys, lungs, and spleens, was different. Concentrations of epirubicin in various tissues were lower than that in liver tissues. Concentrations of epirubicin in various tissues were highest at 5 minutes after drug administration. In each group, concentrations of epirubicin in all tissues, except the spleen, at all time points were lowest in EPI-BCA-MNPS+MF group. Concentrations of epirubicin in the EPI-PBCA-MNPS group and EPI-PBCA-MNPS+MF group were significantly lower than that in EPI group ($p < 0.05$). There were no differences in concentrations of epirubicin in spleens among the groups. There were no differences in concentrations of epirubicin in plasma, hearts, kidneys, lungs, and spleens between the EPI-PBCA-MNPS group and EPI-PBCA-MNPS+MF group ($p > 0.05$). Results analysis showed that epirubicin concentrations in each tissue peaked at about 5 minutes after drug administration (**Figure 2**). This reflected the redistribution of epirubicin in extrahepatic tissues, indicating that phagocytes in extrahepatic tissues could devour magnetic nanoparticles and enter target liver tissues. Thus, epirubicin

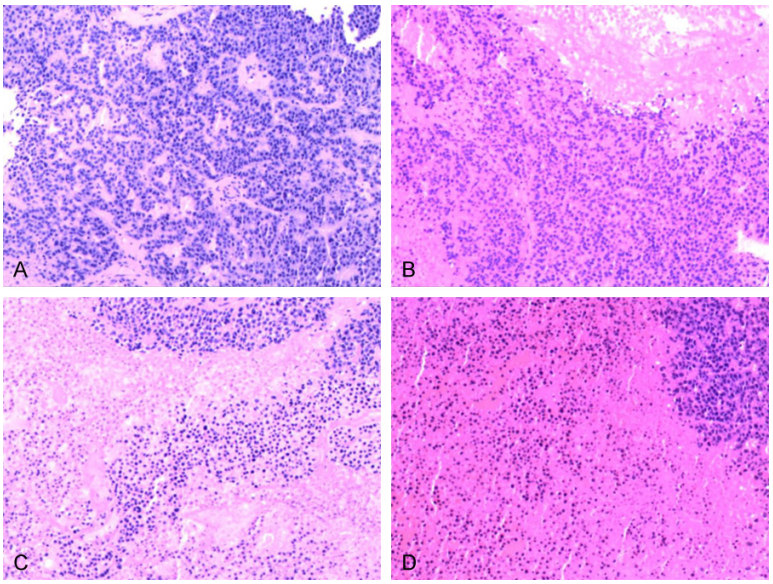

Figure 3. Growth situation of tumor cells in orthotopically transplanted tumor in nude mice under the microscope after drug administration, A. After 2 weeks of treatment, tumor cells in the control group (NS group) still proliferated actively and no necrosis was observed; B. After 2 weeks of treatment, partial necrosis was observed in the tumor cells in the EPI group; C. After 2 weeks of treatment, severe necrosis was seen in all tumor cells in the EPI-PBCA-MNPS group a; D. After 2 weeks of treatment, significant necrosis was seen in tumor cells in EPI-PBCA-MNPS+MF group and severe necrosis was predominant. Moreover, necrosis was concentrated on the area wherein the magnet was placed and mild necrosis was rare.

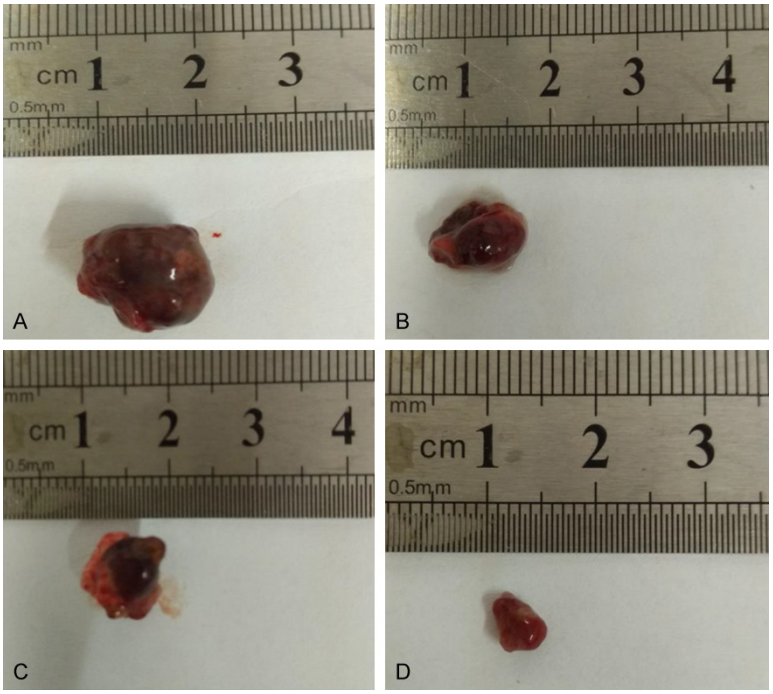

Figure 4. Liver tumor volume in nude mice of each group after drug administration Tumor volume in control group (NS group, A) was largest, followed by tumor volumes in EPI group (B) and EPI-PBCA-MNPS group (C), and the tumor volume in EPI-PBCA-MNPS+MF group (D) was smallest.

concentrations in extrahepatic tissues were significantly reduced.

Establishment of mouse model of human liver cancer and inhibition of EPI-PBCA-MNPS+MF on growth of orthotopically implanted tumors

One mouse died during the preparation of orthotopically transplanted tumors of human liver cancer. One mouse died in the culture process in the EPI group. The animal model was successfully established in 39 mice. After 2 weeks of culturing, the nude mice were sacrificed and dissected. Tumor growth was observed within the livers of nude mice in all groups, except for one mouse with lung metastasis in the NS group. No metastasis was observed in the other groups. Gross anatomy of liver tumors in nude mice: the morphology of liver tumors was regular and tumors were enveloped and lobulated, with a milky white section. H & E staining of various tissues after drug administration revealed that necrosis was seen in tumor tissues, except those in the control group (NS group). Partial necrosis was seen in tumor cells in the EPI group. Severe necrosis was seen in tumor cells in the EPI-PBCA-MNPS group. Significant necrosis was seen in tumor cells in EPI-PBCA-MNPS+MF group and severe necrosis was predominant. Moreover, the necrosis was concentrated on the side where the magnet was placed. Mild necrosis was rare (**Figure 3**).

Liver tumors in nude mice were dissected, except for those in the NS group (contr-

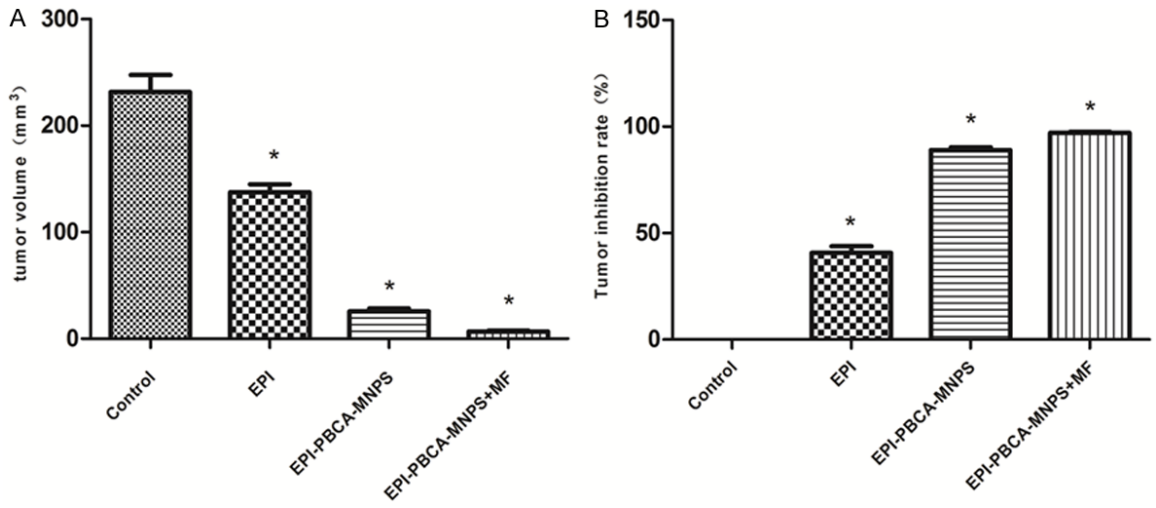

Figure 5. Status on increase and inhibition of liver tumor volume in nude mice after drug administration. A. Statuses on net increase in tumor volume. Increase in tumor volume in EPI group was largest and the increase in tumor volume in EPI-PBCA-MNPS group was larger, while the increase in tumor volume in EPI-PBCA-MNPS+MF group was smallest. B. Status on tumor inhibition rate Compared to the NS group, the tumor inhibition rate was lowest in EPI group, slightly higher in EPI-PBCA-MNPS group, and highest in EPI-PBCA-MNPS+MF group (*, $p < 0.05$).

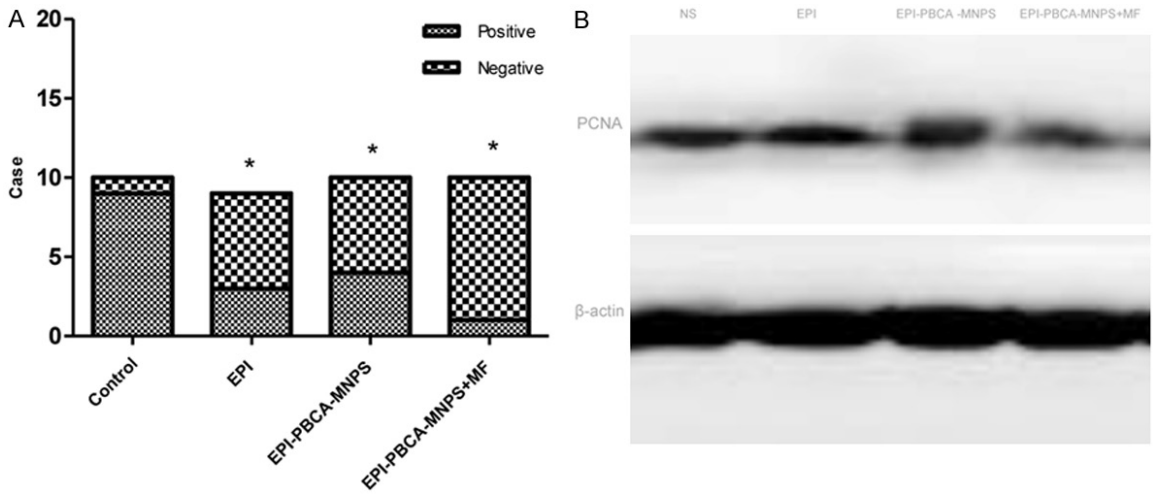

Figure 6. Western-blot detection of expression levels of PCNA protein in orthotopically transplanted tumors in each group. A. Qualitative comparison showed that compared with the NS group, expression of PCNA protein was decreased in EPI group, obviously decreased in the EPI-PBCA-MNPS group, and lowest in EPI-PBCA-MNPS+MF group. Differences in positive PCNA protein rates were statistically significant among the four groups; B. Grayscale analysis showed that the development gradually decreased and was worst in EPI-PBCA -MNPS+MF group. (*, $p<0.05$).

ol group). All transplanted tumors of human liver cancer in nude mice in the other groups were inhibited to varying degrees. Of which, the lengths of tumors were measured and compared among groups with a Vernier caliper. Lengths of tumors were greatest in the EPI group and smallest in EPI-PBCA-MNPS+MF group (**Figure 4**). Increase in tumor volume in the EPI group (137.40±22.41) was greatest and the inhibition rate was lowest (40.64±9.68). Tumor volume in the EPI-PBCA-MNPS group was smaller than that in EPI group (25.58±8.64). Inhibition rate in the EPI-PBCA-MNPS group was slightly higher than that in EPI group (88.95±3.73). Increase in tumor volume (6.66±2.80) was smallest and inhibition rate was highest (97.12±1.21) in the EPI-PBCA-MNPS+MF group. There were statistically significant differences among the four groups ($p < 0.05$) (**Figure 5**).

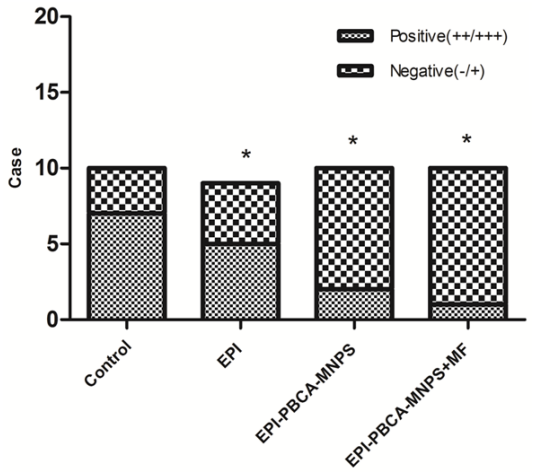

Figure 7. Immunohistochemistry detection of expression of PCNA in liver tumor tissue of nude mice. More than 50% tumor cells in NS group (70%) and EPI group (55.56%) had positive PCNA protein expression. Positive expression of PCNA protein was 20% in the EPI-PBCA-MNPS group; while the positive cells with expression of PCNA protein in the EPI-PBCA-MNPS+MF group (10%) was decreased significantly, there was a statistically significant difference among four groups (*, $p < 0.05$).

Inhibition of EPI-PBCA-MNPS+MF on expression of PCNA in nude mouse liver tumors

β-actin was taken as an internal reference. Expression of PCNA protein in the EPI group (66.67%) was significantly lower than that in NS group (control group, 90%). Expression of PCNA protein in the EPI-PBCA-MNPS group (40%) and EPI-PBCA-MNPS+MF group (10%) decreased gradually, but expression of PCNA protein in the latter was lower. Differences were statistically significant among the four groups ($X^2 = 35.482$, $p < 0.01$) (**Figure 6**).

Immunohistochemical results (magnification 400×) revealed that more than 50% of tumor cells in the NS group (70%) and EPI group (55.56%) had positive PCNA protein expression. Positive expression of PCNA protein was 20% in the EPI-PBCA-MNPS group, while positive cells with expression of PCNA protein in the EPI-PBCA-MNPS+MF group (10%) was decreased significantly. There were statistically significant differences among the four groups ($p < 0.05$) (**Figure 7**). PCNA protein was highly expressed in liver tumors of nude mice in the NS (control) group and more scattered significant hyperchromatic nuclei were observed. PCNA protein was also highly expressed in liver tumors of nude mice in the EPI group, lower than that in control group. More scattered significant hyperchromatic nuclei were also observed. Expression of PCNA protein was significantly decreased in liver tumors of nude mice and less scattered significant hyperchromatic nuclei were observed. Expression of PCNA protein was lowest in liver tumors of nude mice in the EPI-PBCA-MNPS+MF group and least hyperchromatic nuclei were concentrated on the side where the magnet was placed (**Figure 8**).

Discussion

The present study demonstrated that EPI-PBCA-MNPS had the best liver targeting ability under an applied magnetic field. Its concentration in the hepatic region was higher than the concentration of epirubicin in non-target hepatic region ($p < 0.05$). Epirubicin can be slowly released in the liver after being encapsulated in the nanoparticles. The drug concentration and half-life period in the liver are further prolonged. Therefore, dosages of epirubicin can be decreased for patients with liver cancer that are undergoing chemotherapy, reducing side effects. In addition, concentrations of epirubicin in the plasma were decreased after drug administration through tail veins, indicating that phagocytes in the plasma engulfed the magnetic nanoparticles and entered the target organ (liver). In the EPI-PBCA-MNPS group, concentrations of epirubicin in the liver were significantly increased. Peak drug concentration was advanced to 5 minutes after drug administration and concentrations of epirubicin in etrahepatic organs such as hearts, lungs, spleens, and kidneys were further decreased. Examination of tumor volume in nude mice showed that tumor volume in the NS group was largest, while tumor volume in the EPI-PBCA-MNPS+MF group was smallest ($p < 0.05$). Differences among the groups were statistically significant ($p < 0.05$), indicating that EPI-PBCA-MNPS has significant inhibitory effects on tumor growth and can inhibit further tumor growth under an external magnetic field. These results are completely consistent with the result that tumor volume inhibition rate of EPI-PBCA-MNPS under an external magnetic field was highest, indicating that EPI-PBCA-MNPS has good magnetic inductive capacity. Drug retention in the capillaries is very important. In the magnetic field, the capillary blood flow velocity of the target region can be slowed down or even stopped, hence EPI concentra-

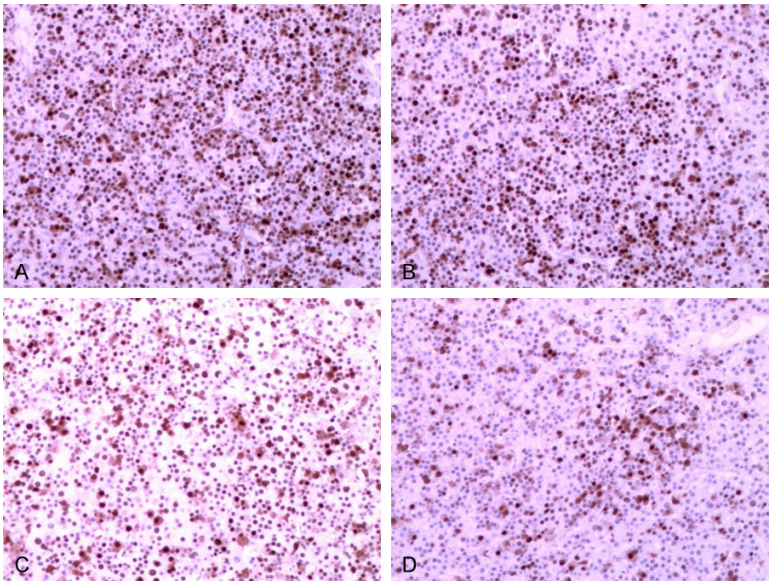

Figure 8. PCNA expression revealed by immunohistochemistry staining (magnification 400 ×). A. PCNA protein was highly expressed in liver tumors of nude mice in NS (control) group and more scattered significant hyperchromatic nuclei were observed; B. PCNA protein was also highly expressed in liver tumors of nude mice in EPI group, which was lower than that in control group, and more scattered significant hyperchromatic nuclei were also observed; C. Expression of PCNA protein was significantly decreased in liver tumors of nude mice in EPI-PBCA-MNPS group, and less scattered significant hyperchromatic nuclei were observed; D. Expression of PCNA protein was lowest in liver tumor of nude mice in EPI-PBCA-MNPS+MF group, and least hyperchromatic nuclei were concentrated on the side where the magnet was placed.

tions around tumor tissues are increased. This indicates that the magnetic field is necessary for maintaining high drug concentrations in local tumor tissues, effectively extending the duration of effects of drugs on tumor cells [19]. In addition, EPI-PBCA-MNPS can effectively increase the concentration of drugs in the target hepatic region and decrease the concentration of drugs in extrahepatic tissue in a magnetic field environment. Moreover, drugs can be released slowly and exert effects continuously. Additionally, it can cause capillary embolisms around tumors in the magnetic field environment. This, in turn, causes tumor necrosis and necrosis, thereby increasing the duration of effects of chemotherapeutic drugs on tumor tissues and drug sensitivity [20, 21]. Therefore, liver targeted EPI-PBCA-MNPS, synthesized by modern targeting drug preparation technology, was used to increase the drug concentration in target livers and significantly reduce the drug concentration in extrahepatic organs under the action of an applied magnetic field. In addition, drugs can be slowly released to exert a sustained effect, reducing side effects.

Many transplanted tumor models are currently used in research. These models provide an ideal tool for tumor growth and screening of antitumor drugs. The more classic model is the subcutaneously transplanted tumor animal model. This kind of model still has many problems due to lack of a microenvironment that simulates the microenvironment for real tumor growth. Based on abovementioned studies, the nude mouse models bearing orthotopically transplanted tumors of human liver cancer were established in this study. This model not only retained the biological features of the original tumors but also displayed malignant biological behaviors and characteristics similar to those of *in vivo* human tumors. Du et al. used liposomes composed of phosphatidylcholine to encapsulate the adriamycin. When concentrations of HepG2 cells in liver cancer are four times the drug concentration, adriamycin magnetic nanoparticles can accumulate at the tumor site under the action of a magnetic field [22]. Mancarella et al. also injected Fe_3O_4 magnetic nanoparticles loaded with antibodies into mice with colon cancers. They found that more magnetic nanoparticles accumulated in the tumor site, while small amounts of magnetic nanoparticles accumulated in other sites [23]. Li et al. analyzed the original expression of tumor cell surface antigens by binding antibodies to Fe_3O_4 magnetic nanoparticles, further indicating that the method has potential application prospect in quantitative detection and analysis of surface antigens [24].

In the present study, EPI injections were taken as a control. It was found that EPI-PBCA-MNPS had obvious anti-tumor effects on orthotopically transplanted liver cancer in nude mice. Because expression of PCNA is related to changes in cell cycles, the activity of cell prolif-

eration can be estimated according to the expression level of PCNA. In this study, both immunohistochemistry and Western blotting showed that the EPI-PBCA-MNPS+MF group had lowest expression of PCNA protein in transplanted liver cancer in nude mice ($p < 0.05$), confirming that EPI-PBCA-MNPS+MF can inhibit cell cycle transformation of liver cancer cells *in vivo*, thus inhibiting the growth of liver cancer cells. Additionally, it was suggested that EPI injections had no significant effects on growth of transplanted tumors. The possible reason is that it is degraded and metabolized *in vivo* in the transportational process. EPI-PBCA-MNPS has liver targetability and can reach the liver tissue and is less degraded. Also, it can inhibit proliferation of malignant tumor cells in the magnetic field environment, change the function of tumor cell membrane, affect cell membrane permeability, and enhance the cytotoxic effects of anti-cancer drugs [25]. Therefore, it was speculated that EPI-PBCA-MNPS can inhibit the malignant proliferation of liver cancer cells *in vivo*. This may be one of the mechanisms for inhibiting tumor growth.

In tumor chemotherapy, to minimize the toxic and side effects of chemotherapeutic drugs, it is required that drugs can not only accumulate in the target organs but also around the tumor. This helps to achieve the maximum effects of chemotherapeutic drugs. This experimental study showed that, after the use of magnetic nanoparticles plus magnetic field, epirubicin concentrations in livers were further increased, higher than that in the non-target hepatic region and those in other two groups ($p < 0.05$). This indicates that the applied magnetic field is effective in improving the target distribution of magnetic drugs in the liver. The prepared EPI-PBCA-MNPS had good magnetic induction ability. Drug retention in the capillaries is very important. Magnetic nanoparticles retained in the capillaries can aggregate with each other under the influence of applied magnetic fields [26, 27]. In the magnetic field, the capillary blood flow velocity of the target region can be slowed down or even stopped, hence the EPI concentration around the tumor tissue is increased, indicating that the external magnetic field is necessary for maintaining high drug concentrations in local tumor tissues. This can effectively extend the duration of effects of drugs on tumor cells and is very important for effective killing of tumor cells [28, 29]. Therefore, EPI-PBCA-MNPS can increase drug concentrations in target livers and significantly reduce the drug concentrations in extrahepatic organs under the action of applied magnetic field. In addition, this drug can be slowly released to exert a sustained effect. Consequently, this distribution mode can not only maintain high drug concentrations in areas of primary tumors but also maintain relatively high drug concentrations in areas of other metastases within the liver to achieve the best anticancer effects.

In summary, EPI-PBCA-MNPS has good magnetic induction and liver targeting. EPI-PBCA-MNPS intravenously injected in rats in the magnetic field environment can significantly increase concentrations of epirubicin in target hepatic regions and further reduce concentrations of epirubicin in other non-target hepatic regions. In a magnetic field environment, EPI-PBCA-MNPS can significantly inhibit transplanted tumors of human liver cancers in animal models. Additionally, it has highly targeted treatment effects and low toxicity. It can improve the survival rates and survival times of tumor-bearing animals, thus providing new chemotherapeutic agents and treatment methods for clinical treatment of unresectable liver cancers and metastases.

Acknowledgements

The present review was supported by awards from the Nantong Science and Technology Foundation of China (grant no. MS12015057).

Disclosure of conflict of interest

None.

Address correspondence to: Jin-Zhu Wu, Department of Hepatobiliary Surgery, Nantong Institute of Liver Disease, Nantong Third People's Hospital, Nantong University, No. 60 Middle Qing Nian Road, Nantong 226006, Jiangsu, China. E-mail: wujinzhu-19821124@sina.com

References

[1] Shen JM, Li XX, Fan LL, Zhou X, Han JM, Jia MK, Wu LF, Zhang XX and Chen J. Heterogeneous dimer peptide-conjugated polylysine dendrimer-Fe3O4 composite as a novel nanoscale molecular probe for early diagnosis and therapy in hepatocellular carcinoma. Int J Nanomedicine 2017; 12: 1183-1200.

[2] Li JJ, Chen T, Deng F, Wan JY, Tang YL, Yuan P and Zhang LK. Synthesis, characterization, and in vitro evaluation of curcumin-loaded albumin nanoparticles surface-functionalized with glycyrrhetinic acid. Int J Nanomedicine 2015; 10: 5475-5487.
[3] Salatin S and Yari Khosroushahi A. Overviews on the cellular uptake mechanism of polysaccharide colloidal nanoparticles. J Cell Mol Med 2017; 21: 1668-1686.
[4] Siafaka PI, Okur NÜ, Karavas E and Bikiaris DN. Surface modified multifunctional and stimul responsive nanoparticles for drug targeting: current status and uses. Int J Mol Sci 2016; 17: 1440.
[5] Feng XL, Chen AJ, Zhang YL, Wang JF, Shao LQ and Wei LM. Central nervous system toxicity of metallic nanoparticles. Int J Nanomedicine 2015; 10: 4321-4340.
[6] Yhee JY, Im J and Nho RS. Advanced therapeutic strategies for chronic lung disease using nanoparticle-based drug delivery. J Clin Med 2016; 5: 82.
[7] Baetke SC, Lammers T and Kiessling F. Applications of nanoparticles for diagnosis and therapy of cancer. Br J Radiol 2015; 88: 20150207.
[8] Ensign LM, Cone R and Hanes J. Nanoparticle-based drug delivery to the vagina: a review. J Control Release 2014; 190: 500-514.
[9] Siddiqi KS, Ur RA, Tajuddin and Husen A. Biogenic fabrication of iron/iron oxide nanoparticles and their application. Nanoscale Res Lett 2016; 11: 498.
[10] Prabhu RH, Patravale VB and Joshi MD. Polymeric nanoparticles for targeted treatment in oncology: current insights. Int J Nanomedicine 2015; 10: 1001-1018.
[11] Li J, Zhang YD, Zhao JF, Yang P and Duan JH. Targeting therapy with epirubicin polybutylcyanoacrylate magnetic nanoparticles for transplanted hepatoma in nude mice. CHIN J Exp Surg 2011; 28: 1111-1114.
[12] Zhou HG, Tang JL, Li JY, Li WQ, Liu Y and Chen CY. In vivo aggregation-induced transition between T1 and T2 relaxations of magnetic ultrasmall iron oxide nanoparticles in tumor microenvironment. Nanoscale 2017; 9: 3040-3050.
[13] Varshosaz J and Farzan M. Nanoparticles for targeted delivery of therapeutics and small interfering RNAs in hepatocellular carcinoma. World J Gastroenterol 2017; 21: 12022-12041.
[14] Moradzadeh Khiavi M, Rostami A, Hamishekar H, Mesgari Abassi M, Aghbali A, Salehi R, Abdollahi B, Fotoohi S and Sina M. Therapeutic efficacy of orally delivered doxorubicin nanoparticles in rat tongue cancer induced by 4-nitroquinoline 1-oxide. Adv Pharm Bull 2015; 5: 209-216.
[15] Horák D, Pustovyy VI, Babinskyi AV, Palyvoda OM, Chekhun VF, Todor IN and Kuzmenko OI. Enhanced antitumor activity of surface-modified iron oxide nanoparticles and an α-tocopherol derivative in a rat model of mammary gland carcinosarcoma. Int J Nanomedicine 2017; 12: 4257-4268.
[16] Lee CY and Ooi IH. Preparation of temozolomide-loaded nanoparticles for glioblastoma multiforme targeting-ideal versus reality. Pharmaceuticals B 2016; 9: 54.
[17] Wang X, Low XC, Hou W, Abdullah LN, Toh TB, Mohd Abdul Rashid M, Ho D and Chow EK. Epirubicin-adsorbed nanodiamonds kill chemoresistant hepatic cancer stem cells. ACS Nano 2014; 8: 12151-12166.
[18] Perçin I, Karakoç V, Ergün B and Denizli A. Metal-immobilized magnetic nanoparticles for cytochrome C purification from rat liver. Biotechnology 2016; 63: 31-40.
[19] Melguizo C, Cabeza L, Prados J, Ortiz R, Caba O, Rama AR, Delgado ÁV and Arias JL. Enhanced antitumoral activity of doxorubicin against lung cancer cells using biodegradable poly (butylcyanoacrylate) nanoparticles. Drug Des Devel Ther 2015; 9: 6433–6444.
[20] Laffon B, Fernández-Bertólez N, Costa C, Brandão F, Teixeira JP, Pásaro E and Valdiglesias V. Cellular and molecular toxicity of iron oxide nanoparticles. Adv Exp Med Biol 2018; 1048: 199-213.
[21] Rasaneh S, Rajabi H and Johari Daha F. Activity estimation in radioimmunotherapy using magnetic nanoparticles. Chin J Cancer Res 2015; 27: 203-208.
[22] Du X, Zhou J, Wu L, Sun S and Xu B. Enzymatic transformation of phosphate decorated magnetic nanoparticles for selectively sorting and inhibiting cancer cells. Bioconjug Chem 2014; 25: 2129-2133.
[23] Mancarella S, Greco V, Baldassarre F, Vergara D, Maffia M and Leporatti S. Polymer-coated magnetic nanoparticles for curcumin delivery to cancer cells. Macromol Biosci 2015; 15: 1365-1374.
[24] Li YJ, Dong M, Kong FM and Zhou JP. Folate-decorated anticancer drug and magnetic nanoparticles encapsulated polymeric carrier for liver cancer therapeutics. Int J Pharm 2015; 489: 83-90.
[25] Rasaneh S, Rajabi H and Johari DF. Activity estimation in radioimmunotherapy using magnetic nanoparticles. Chin J Cancer Res 2015; 27: 203-208.
[26] Estelrich J, Escribano E, Queralt J and Busquets MA. Iron oxide nanoparticles for magnetically-guided and magnetically-responsive drug delivery. Int J Mol Sci 2015; 16: 8070-8101.

[27] Gobbo OL, Sjaastad K, Radomski MW, Volkov Y and Prina-Mello A. Magnetic nanoparticles in cancer theranostics. Theranostics 2015; 5: 1249-1263.

[28] Próspero AG, Quini CC, Bakuzis AF, Fidelis-de-Oliveira P, Moretto GM, Mello FP, Calabresi MF, Matos RV, Zandoná EA and Zufelato N. Real-time in vivo monitoring of magnetic nanoparticles in the bloodstream by AC biosusceptometry. J Nanobiotechnology 2017; 15: 22.

[29] Coricovac DE, Moacă EA, Pinzaru I, Cîtu C, Soica C, Mihali CV, Păcurariu C, Tutelyan VA, Tsatsakis A and Dehelean CA. Biocompatible colloidal suspensions based on magnetic iron oxide nanoparticles: synthesis, characterization and toxicological profile. Front Pharmacol 2017; 8: 154.